

12

AFWAL-TR-82-4053



GENERAL RELATIONS FOR EXACT AND INEXACT INVOLUTE BODIES OF REVOLUTION

NICHOLAS J. PAGANO
MECHANICS AND SURFACE INTERACTIONS BRANCH
NONMETALLIC MATERIALS DIVISION

April 1982

Interim Report
August 1981 - February 1982

DTIC
ELECTE
FEB 24 1983
S B

Approved for public release; distribution unlimited.

MATERIALS LABORATORY
AIR FORCE WRIGHT AERONAUTICAL LABORATORIES
AIR FORCE SYSTEMS COMMAND
WRIGHT-PATTERSON AIR FORCE BASE, OHIO 45433

83 02 023 169

AD A 1 2 4 8 4 9

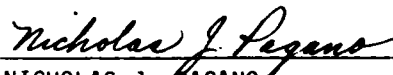
DTIC FILE COPY

NOTICE

When Government drawings, specifications, or other data are used for any purpose other than in connection with a definitely related Government procurement operation, the United States Government thereby incurs no responsibility nor any obligation whatsoever; and the fact that the Government may have formulated, furnished, or in any way supplied the said drawings, specifications, or other data, is not to be regarded by implication or otherwise as in any manner licensing the holder or any other person or corporation, or conveying any rights or permission to manufacture, use, or sell any patented invention that may in any way be related thereto.

This report has been reviewed by the Office of Public Affairs (ASD/PA) and is releasable to the National Technical Information Service (NTIS). At NTIS, it will be available to the general public, including foreign nations.

This technical report has been reviewed and is approved for publication.



NICHOLAS J. PAGANO
Materials Research Engineer
Mechanics & Surface Interactions Branch
Nonmetallic Materials Division



STEPHEN W. TSAI, Chief
Mechanics & Surface Interactions Branch
Nonmetallic Materials Division

FOR THE COMMANDER



FRANKLIN D. CHERRY, Chief
Nonmetallic Materials Division

"If your address has changed, if you wish to be removed from our mailing list, or if the addressee is no longer employed by your organization please notify AFWAL/MLBM, W-PAFB, Ohio 45433 to help us maintain a current mailing list.

Copies of this report should not be returned unless return is required by security considerations, contractual obligations, or notice on a specific document.

Unclassified

SECURITY CLASSIFICATION OF THIS PAGE (When Data Entered)

REPORT DOCUMENTATION PAGE		READ INSTRUCTIONS BEFORE COMPLETING FORM
1. REPORT NUMBER AFWAL-TR-82-4053	2. GOVT ACCESSION NO. AD-A124 849	3. RECIPIENT'S CATALOG NUMBER
4. TITLE (and Subtitle) GENERAL RELATIONS FOR EXACT AND INEXACT INVOLUTE BODIES OF REVOLUTION	5. TYPE OF REPORT & PERIOD COVERED Interim Report August 1981 - February 1982	
	6. PERFORMING ORG. REPORT NUMBER	
7. AUTHOR(s) Nicholas J. Pagano	8. CONTRACT OR GRANT NUMBER(s)	
9. PERFORMING ORGANIZATION NAME AND ADDRESS Materials Laboratory (AFWAL/MLBM) Air Force Systems Command Wright-Patterson AFB, OH 45433	10. PROGRAM ELEMENT, PROJECT, TASK AREA & WORK UNIT NUMBERS 2307P115	
11. CONTROLLING OFFICE NAME AND ADDRESS Materials Laboratory (AFWAL/MLBM) Air Force Wright Aeronautical Laboratories Wright-Patterson AFB, OH 45433	12. REPORT DATE April 1982	
	13. NUMBER OF PAGES 38	
14. MONITORING AGENCY NAME & ADDRESS (if different from Controlling Office)	15. SECURITY CLASS. (of this report) Unclassified	
	15a. DECLASSIFICATION DOWNGRADING SCHEDULE	
16. DISTRIBUTION STATEMENT (of this Report) Approved for public release; distribution unlimited.		
17. DISTRIBUTION STATEMENT (of the abstract entered in Block 20, if different from Report)		
18. SUPPLEMENTARY NOTES		
19. KEY WORDS (Continue on reverse side if necessary and identify by block number) Exact Involute Surface Rocket Nozzles Fabric Distortion Exit Cones Interleaf Involutes Carbon-Carbon Exit Cones Ply Patterns Debulk Kinematics Start-Line Method		
20. ABSTRACT (Continue on reverse side if necessary and identify by block number) A thorough treatment of the mathematical modeling characterizing various aspects of involute construction geometry is presented in this report. Included in the work are the equations that describe the exact involute approach as well as the so called start-line method which contains certain approximations. New features incorporated include the treatment of interleaf ply patterns, kinematics of debulking, errors caused by the approximations in the start-line approach in terms of discontinuity strains, and explicit (closed form) relations that characterize the hypothetical involute surface in the latter approach. The \rightarrow over		

DD FORM 1 JAN 73 1473

EDITION OF 1 NOV 65 IS OBSOLETE

Unclassified

SECURITY CLASSIFICATION OF THIS PAGE (When Data Entered)

Unclassified

SECURITY CLASSIFICATION OF THIS PAGE(When Data Entered)

equations presented also provide a complete description of the involute surface geometric parameters necessary to define the distribution of the elastic stiffness tensor.



Unclassified

SECURITY CLASSIFICATION OF THIS PAGE(When Data Entered)

INTRODUCTION

An exact involute surface (EIS) is defined by the relation [1]

$$r \sin \alpha = c \quad (1)$$

where r is the radial coordinate, α is the arc angle, and c is called the involute constant. Angular coordinate θ is given by

$$\theta - \theta_0 = \frac{A}{c} (z - z_0) + \alpha_0 + \cot \alpha_0 - \alpha - \cot \alpha \quad (2)$$

where the point defined by $r = r_0$ ($\alpha = \alpha_0$), $\theta = \theta_0$, $z = z_0$ is simply a base point on the EIS and A is a constant related to the number of plies N , ply thickness t , and constant c by

$$A = \left(\frac{4\pi^2 c^2}{N^2 t^2} - 1 \right)^{\frac{1}{2}} \quad (3)$$

The positive directions of the various geometric variables are shown in Figure 1*, where it should be noted that the (θ, r, z) axes form a right-handed triad.

Other important geometric parameters of the EIS are the tilt angle γ , surface angle ψ , and helical angle ϕ , which are shown in their positive directions in Figure 2. These are defined by

$$\tan \gamma = \frac{dr}{dz} = \frac{A}{\cos \alpha} \quad (4)$$

$$\cos \psi = -\sin \alpha \sin \gamma \quad (5)$$

and

$$\phi = \phi_0 + \psi_0 - \psi + \frac{A}{(A^2 + 1)^{\frac{1}{2}}} \left[\frac{A}{c} (z - z_0) + \cot \alpha_0 - \cot \alpha \right] \quad (6)$$

where ϕ represents the angle from the local meridional direction to a line in the EIS that was originally straight (in the ply pattern), such as the warp direction, and ϕ_0 is the corresponding angle at the base point.

*Figures are located at end of report.

The developed configuration (or ply pattern) of the EIS is defined by the parametric relations

$$\tan \lambda = \frac{c}{A} \left(\frac{A^2+1}{r^2-c^2} \right)^{1/2} \quad (7)$$

$$\theta = \frac{A^2 z}{c(A^2+1)^{1/2}} - \lambda - \cot \lambda \quad (8)$$

$$R = \frac{1}{A^2} [(A^2+1)(A^2 r^2 + c^2)]^{1/2} \quad (9)$$

where the ply pattern coordinates R, θ are shown in Figure 3.

The foregoing equations, (1) - (9), completely define the configuration of the EIS and its ply pattern, and require only the prescription of constants c, N, t (or equivalent information), initial values θ_0 , ϕ_0 , and the r, z profile of the body of revolution being generated by the involute method. The body of revolution itself need only possess piecewise-continuous boundaries. Equations (1) - (9) guarantee that the volume of the body will be completely and perfectly filled by layers of ideally flexible material having constant thickness (aside from highly-localized boundary regions where the thickness varies to avoid "steps"). However, exact involute construction is not widely used in the manufacture of practical components, such as rocket nozzle exit cones. Rather, various ply pattern models based upon analytical and empirical methods are employed, including interleaving, which consists of the use of plies of (usually) two different shapes and thicknesses in the same body. Thus, it is important to mathematically describe the geometry and to define relations that measure the degree of error induced via these approximate methods, which is the purpose of the present communication.

A comment on the organization of this report is in order at this time. In the next section, we shall present the equations that define the involute surface, i.e., the three-dimensional surface formed by a ply within the body of revolution, and the associated ply pattern according to contemporary procedure [2, 3, 4]. This procedure consists of the analysis of involute surface "strips" of finite dimension and involves iterative solutions of the basic equations. Some new results for the description of the helical angle distribution and ply pattern analysis in the presence of interleaving are also given there. New work that leads to precise (closed form) solutions of the basic equations is presented in a subsequent section. This is done in the interest of clarity, and also to establish a complete formulation by the finite strip method since the ply pattern analysis does not lead to a convenient closed representation.



Accession For	
NTIS GRA&I	<input checked="" type="checkbox"/>
DTIC TAB	<input type="checkbox"/>
Unannounced	<input type="checkbox"/>
Justification	
By _____	
Distribution/	
Availability Codes	
Dist	Avail and/or Special
A	

THE START-LINE METHOD

a) INVOLUTE SURFACE STRIP

The model employed herein assumes that the involute surface consists of strips, each of which obeys eqs. (1) - (9) with piecewise constant c , such that consecutive strips are continuous at a single point. The consecutive strips possess a common terminal plane $z = \text{constant}$. This model leads to perfect filling of volume if the strip dimension is infinitesimal but results in discontinuities in the form of "plateaus" in the involute surface. Furthermore, we introduce the concept of a start-line, as described by Savage [3] and Stanton [4] to control the local orientation of the involute surface. The start-line is simply a meridian ($\theta = \text{constant}$) of the involute surface and is only required to be piecewise-continuous. It seems that most, if not all, of the ply pattern design approaches used in practice can be derived by appropriate tailoring of the start-line [4]. Furthermore, we shall use the term hypothetical involute surface to refer to the involute surface conceived in the start-line method, which cannot be formed from sheets of continuous material because of the discontinuities required. It will be necessary to refer to four specific values of radius; namely, inner and outer radii r_I and r_O , respectively, start-line radius r_S , and for the case where interleaving is present, r_C is the intersection of two regions having different values of N and t . Each of the four radii are functions that depend on axial coordinate z . Since the constants N and t usually appear in the form of their product, we let

$$M = Nt \quad (10)$$

We shall consider a strip of the involute surface as the region formed by $z_1 \leq z \leq z_2$. Parameters will carry a subscript q ($q = 1, 2$) that corresponds to thickness parameter M if interleaving is present. Our convention¹ is that $q = 1$ corresponds to the region $r > r_C$ if $r_S > r_C$ and $r \leq r_C$ otherwise. We cannot permit the quantity $r_S - r_C$ to change sign in a given problem, although it may vanish. Also, a subscript G ($G = I, O, S, C$) will be used to refer to any of the four special values of r discussed above. If the value of r is arbitrary, no G subscript will be displayed. It will also be understood that, unless otherwise noted, the following equations are only valid within a single strip, hence no index for strip identification will be employed unless needed for clarity. Finally, we introduce the representation $F_{Gq}(z_j, z_k) = \alpha_{Gq}(z_j) + \cot \alpha_{Gq}(z_j) - \alpha_{Gq}(z_k) - \cot \alpha_{Gq}(z_k)$ (11) and we assume that $r_S(z_2) - r_S(z_1)$ is not negative.

We now let the strip geometry be defined by the governing involute equation

$$r \sin \alpha_q = c_q \quad (12)$$

where c_q is piecewise-constant. While r , θ , and z are all continuous at $r = r_C$, arc angle α is discontinuous there. We also let

$$A_q = \left(\frac{4\pi^2 c_q^2}{M_q^2} - 1 \right)^{\frac{1}{2}} \quad (13)$$

The constants c_q cannot be arbitrarily prescribed when using the start-line approach. Rather, c_1 is computed such that it satisfies

$$F_{S1}(z_1, z_2) = \frac{A_1}{c_1} (z_1 - z_2) \quad (14)$$

¹Interleaf terminations on planes $z = \text{const.}$ are not treated in this work.

in conjunction with (12) and (13) with $q = 1$. These relations guarantee that the points on the hypothetical involute surface corresponding to $r = r_S$ at $z = z_1, z_2$ lie on the same meridian $\theta = \theta_S$. A good first approximation for the solution of this system of equations is given by

$$c_1^2 \approx \frac{1 + p_S^2}{4\pi^2/M_1^2 + p_S^2/r_S^2} \quad (15)$$

where

$$p_G = \frac{r_G(z_2) - r_G(z_1)}{z_2 - z_1} \quad (16)$$

and the subscript G has the same meaning described earlier.

The constants c_2 are governed by continuity of the hypothetical involute surface at $r = r_C, z = z_1, z_2$, which lead to

$$F_{C2}(z_1, z_2) - F_{C1}(z_1, z_2) = \left(\frac{A_2}{c_2} - \frac{A_1}{c_1}\right)(z_1 - z_2) \quad (17)$$

along with (12) and (13). We may use

$$c_2 \approx \frac{M_2}{M_1} c_1 \quad (18)$$

as a good first approximation for the solution of (17), (12), and (13), although solutions do not exist for arbitrary values of the input parameters. The involute surface strip is thus defined by

$$\begin{aligned} \theta_q(z) = & \theta_S + \frac{A_q}{c_q} (z - z_1) + \alpha_{S1}(z_1) + \cot \alpha_{S1}(z_1) - \alpha_q(z) - \cot \alpha_q(z) \\ & + [\alpha_{C2}(z_1) + \cot \alpha_{C2}(z_1) - \alpha_{C1}(z_1) - \cot \alpha_{C1}(z_1)] \delta_{q2} \end{aligned} \quad (19)$$

which is continuous at $z = z_1, z_2$. Here, δ_{qp} is the Kronecker delta; specifically, $\delta_{22} = 1$ and $\delta_{12} = 0$. The tilt and surface angles, defined . .

$$\tan \gamma_q = \frac{A_q}{\cos \alpha_q} \quad (20)$$

and

$$\cos \psi_q = - \sin \alpha_q \sin \gamma_q \quad (21)$$

like α_q , contain discontinuities at $r = r_C$.

We next consider the distribution of helical angle ϕ , where we restrict our attention to the case in which the warp (and fill) fibers of the regions $q = 1, 2$ in the ply pattern are parallel. Within each region of the hypothetical involute surface, the helical angle is given by an equation of the form (6), however, a discontinuity exists at $r = r_C$. To define the magnitude of the discontinuity, we consider a strip of infinitesimal height such that $z_1 = z$ and $z_2 = z + dz$. In this strip, a crease¹ occurs at $r = r_C$. As one may observe by creasing a piece of lined paper, Ω_q , the angles between the warp direction and crease line on either side of the crease line are equivalent. Letting $(\hat{i}, \hat{j}, \hat{k})$ represent unit vectors along the (θ, r, z) directions, respectively, at r_C , the infinitesimal vector along the crease line is given by

$$\bar{d}\ell = -rd\theta\hat{i} + dr\hat{j} + dz\hat{k} \quad (22)$$

But, differentiation of (19) leads to

$$d\theta = \frac{A_q}{c_q} dz + \cot^2 \alpha_{Cq} d\alpha_{Cq} \quad (23)$$

which, on use of (12), becomes

$$c_q d\theta = A_q dz - \cos \alpha_{Cq} dr \quad (24)$$

Now the unit vectors along the warp direction on either side of r_C are given by \hat{w}_q where (see eqs. 8, 12, 13 of Reference [2])

¹ In actual involute bodies, the crease appears to be smoothed out.

$$\begin{aligned} \hat{w}_q = & \frac{1}{\sin \psi_{Cq}} [\cos \alpha_{Cq} \sin \phi_{Cq} \hat{i} + (\sin \gamma_{Cq} \cos \phi_{Cq} \sin \psi_{Cq} \\ & - \sin \alpha_{Cq} \sin \phi_{Cq} \cos^2 \gamma_{Cq}) \hat{j} + \cos \gamma_{Cq} (\cos \phi_{Cq} \sin \psi_{Cq} \\ & - \cos \psi_{Cq} \sin \phi_{Cq}) \hat{k}] \end{aligned} \quad (25)$$

Letting $\Omega_1 = \Omega_2$, or

$$\bar{d}\ell \cdot \hat{w}_1 = \bar{d}\ell \cdot \hat{w}_2 \quad (26)$$

where the dot signifies a scalar product, leads to the relation

$$f_2 \sin \phi_{C2} + g_2 \cos \phi_{C2} = f_1 \sin \phi_{C1} + g_1 \cos \phi_{C1} \quad (27)$$

where

$$\begin{aligned} f_q = & \frac{1}{\sin \psi_{Cq}} [(\cos \alpha_{Cq} \cot \alpha_{Cq} - \sin \alpha_{Cq} \cos^2 \gamma_{Cq}) p_{C-Aq} \cot \alpha_{Cq} \\ & - \cos \gamma_{Cq} \cos \psi_{Cq}] \end{aligned} \quad (28)$$

$$g_q = \cos \gamma_{Cq} + p_C \sin \gamma_{Cq} \quad (29)$$

recalling that p_C is given by (16). Thus, ϕ_{C2} is defined by the solution of (27), once ϕ_{C1} has been established. The solution of (27) is given by

$$\phi_{C2} = \omega_2 \pm \cos^{-1} \left[\frac{Q_1}{Q_2} \cos (\phi_{C1} - \omega_1) \right] \quad (30)$$

where the positive sign is chosen when $\phi_{C1} \geq \omega_1$, otherwise the negative sign is used. In (30), we have made the replacements

$$\tan \omega_q = \frac{f_q}{g_q} \quad (31)$$

$$Q_q = (f_q^2 + g_q^2)^{1/2} \quad (32)$$

and we have assumed that $0 \leq \phi_{Cq} - \omega_q \leq \pi$.

In the derivation of (30), we have assumed the strip has infinitesimal height $z_2 - z_1 = dz$. For the case of finite height, we use the same relations as an approximation. Furthermore, we choose to write (30) at each point $r_C(z)$ in order to develop the general relation for $\phi_2(z)$, although other interpretations for this approximation are possible, such as writing (30) only at $r_C(z_1)$ and then utilizing an equation of the form (6) for $q = 2$ with base point (r_0, z_0) replaced by $(r_C(z_1), z_1)$. The general expressions for ϕ_q thus become

$$\phi_1(z) = \phi_{S1}(z_1) + \psi_{S1}(z_1) - \psi_1(z) + \frac{A_1}{(A_1^2 + 1)^{\frac{1}{2}}} \left[\frac{A_1}{C_1} (z - z_1) + \cot \alpha_{S1}(z_1) - \cot \alpha_1(z) \right] \quad (33)$$

$$\phi_2(z) = \phi_{C2}(z) + \psi_{C2}(z) - \psi_2(z) + \frac{A_2}{(A_2^2 + 1)^{\frac{1}{2}}} [\cot \alpha_{C2}(z) - \cot \alpha_2(z)] \text{ which follow from (6).}$$

b) PLY PATTERN OF A STRIP

We now turn our attention to the ply pattern, or developed view, of a basic strip of the hypothetical involute surface. For this purpose, we employ a set of equations of the form (7)-(9) to represent each of the mapped regions $q = 1, 2$. In other words, consider two systems of plane cylindrical coordinates (R_q, θ_q) , along with associated parameters λ_q . If the involute construction procedure were exact, we would position the origins and orient the axes of the two coordinate systems such that the ply pattern would be continuous along the crease line. But all solutions other than an exact involute surface are approximate, hence this continuity

condition cannot be perfectly satisfied. Our approach to approximate continuity consists of selecting the two R, θ coordinate systems such that the ply pattern is continuous at the mapped point corresponding to $r_C(z_1)$ while the distance between the two mapped images of $r_C(z_2)$ is minimized. In this manner, three parameters, corresponding to relative translation and rotation of the two coordinate systems, can be evaluated. We shall subsequently employ a similar algorithm to treat strip-to-strip continuity of the ply pattern. Thus, we shall use subscripts a, b in lieu of $1, 2$ in order to avoid specific dependence on the region index q in what follows.

The two plane cylindrical coordinate systems, (R_a, θ_a) and (R_b, θ_b) , are shown in Figure 4(a), as well as a cartesian system (x, y) . For our purposes, we shall regard (x, y) as being fixed in space, while the former two vary in orientation and position according to the strip and region under consideration. From Figure 4(a), we observe that

$$\begin{aligned} x &= \bar{x}_a + R_a \cos(\theta_a - \bar{\theta}_a) = \bar{x}_b + R_b \cos(\theta_b - \bar{\theta}_b) \\ y &= \bar{y}_a + R_a \sin(\theta_a - \bar{\theta}_a) = \bar{y}_b + R_b \sin(\theta_b - \bar{\theta}_b) \end{aligned} \quad (34)$$

for a point P in the ply pattern which has coincident images in the (R_a, θ_a) and (R_b, θ_b) coordinate systems. If the corresponding images of a mapped point do not coincide, they are separated by a distance L which is given by

$$L^2 = [\bar{x}_b - \bar{x}_a + R_b^* \cos(\theta_b^* - \bar{\theta}_b) - R_a^* \cos(\theta_a^* - \bar{\theta}_a)]^2 + [\bar{y}_b - \bar{y}_a + R_b^* \sin(\theta_b^* - \bar{\theta}_b) - R_a^* \sin(\theta_a^* - \bar{\theta}_a)]^2 \quad (35)$$

where we let R_a^* , θ_a^* and R_b^* , θ_b^* represent the mapped coordinates of a point with distinct images. Minimizing the distance L by the operation

$$\frac{\partial L}{\partial (\bar{\theta}_b - \bar{\theta}_a)} = 0 \quad (36)$$

after using (34) to eliminate $\bar{x}_b - \bar{x}_a$ and $\bar{y}_b - \bar{y}_a$, we get

$$\tan (\bar{\theta}_b - \bar{\theta}_a) = \frac{B_1}{B_2} \quad (37)$$

where

$$\begin{aligned} B_1 = & R_a R_b^* \sin(\theta_a - \theta_b^*) + R_a^* R_b \sin(\theta_a^* - \theta_b) + R_a R_b \sin(\theta_b - \theta_a) \\ & + R_a^* R_b^* \sin(\theta_b^* - \theta_a^*) \end{aligned} \quad (38)$$

$$\begin{aligned} B_2 = & - R_a R_b^* \cos(\theta_a - \theta_b^*) - R_a^* R_b \cos(\theta_a^* - \theta_b) + R_a R_b \cos(\theta_b - \theta_a) \\ & + R_a^* R_b^* \cos(\theta_b^* - \theta_a^*) \end{aligned}$$

It should be noted that eq. (37) always has two roots. The correct root is the one which minimizes L in eq. (35).

Thus, to satisfy the aforementioned continuity conditions for adjoining regions $q = 1, 2$, we simply let $a = 1$, $b = 2$ (or vice versa) and make the replacements

$$\begin{aligned} R_q &= R_{Cq}(z_1), \quad \theta_q = \theta_{Cq}(z_1) \\ R_q^* &= R_{Cq}(z_2), \quad \theta_q^* = \theta_{Cq}(z_2) \end{aligned} \quad (39)$$

in (38), which in turn is substituted into (37) and thence into (34), so that the coordinates of the ply pattern strip become

$$x = \bar{x}_q + R \cos (\theta - \bar{\theta}_q) \quad (40)$$

$$y = \bar{y}_q + R \sin (\theta - \bar{\theta}_q)$$

according as the image point (R, θ) corresponds to $q = 1$ or $q = 2$. In (40), we let (R, θ) represent the ply pattern parameters of an arbitrary point, which may lie in either region.

c) SPECIAL CASE: CYLINDRICAL INVOLUTE STRIP

In the usual case, R and θ are given by eqs. (7) - (9). An exceptional case occurs however, when the hypothetical involute surface strip is cylindrical, i.e., $\gamma = A = 0$. In this case, eq. (9) is not valid and the ply pattern degenerates into a trapezoid in which the mapped edges corresponding to the planes $z = \text{constant}$ are parallel. Furthermore, the length of each of these mapped edges is equal to its arc length in the involute surface. Thus, referring to Figure 4(b), we redefine the quantities R and θ for this special case by

$$R_{\text{CYL}}^2(z) = (z-z_1)^2 + \frac{[r^2(z) - r_G^2(z_1)]^2}{4c_q^2} \quad (41)$$

$$\sin \theta_{\text{CYL}}(z) = \frac{|z-z_1|}{R_{\text{CYL}}(z)} \quad (42)$$

where G may be set equal to S if $q = 1$ and C if $q = 2$ for convenience. In this way, the origin of R, θ coordinates in Figure 4(b) is placed at the image of $r_S(z_1)$ if $q = 1$ and $r_C(z_1)$ if $q = 2$. With the interpretation of (41) and (42) for any cylindrical involute region, the previous (and subsequent) ply pattern equations are all valid.

d) CONNECTIVITY OF STRIPS

The preceding equations (10) - (21) define the hypothetical involute surface, or spatial configuration of a ply within the generated body of revolution conceived in the start-line method. As mentioned earlier, the strips are only connected along the start-line itself. Internal continuity conditions between regions $q = 1, 2$ have already been established. Thus, for piecewise-continuous functions $r_G(z)$, these equations represent a complete system. It is only necessary to recall that, for consecutive strips, the previous value of z_2 becomes the new value of z_1 (for the next strip).

In order to define the helical angle distribution via eqs. (33), an additional constraint is required, for example

$$\phi_{S1}^{(i)}(z_2) = \phi_{S1}^{(i+1)}(z_1) \quad (43)$$

where we have introduced a strip index as a superscript since the relation involves consecutive strips. However, because of the inherent approximation of the start-line method, (43) must be viewed as an assumption. It may be just as accurate to assume that $\phi_{S1}(z)$ is a constant. For typical exit cones in which α is quite small, the difference between these two assumptions would be negligible.

Unlike the hypothetical involute surface, however, the ply pattern equations (34) - (42) do require explicit connectivity relations to define strip-to-strip continuity. Here, the above algorithm involving eqs. (38), (37), and (34) is repeated, however, in place of (39) we use

$$\begin{aligned}
R_a^{(i)} &= R_S(z_2), \quad \theta_a^{(i)} = \theta_S(z_2) \\
R_b^{(i+1)} &= R_S(z_1), \quad \theta_b^{(i+1)} = \theta_S(z_1) \\
R_a^* &= R_G(z_2), \quad \theta_a^* = \theta_G(z_2) \\
R_b^* &= R_G(z_1), \quad \theta_b^* = \theta_G(z_1)
\end{aligned} \tag{44}$$

where $G \neq S$ may be chosen arbitrarily. Convenient choices are $G = C$ or $G = I$ or O , corresponding to the farthest point from the start-line. The ply pattern coordinates are thus given by

$$\begin{aligned}
x &\equiv x = \bar{x}_q^{(i)} + R \cos \left(\theta - \frac{(i)}{\theta}_q \right) \\
y &\equiv y = \bar{y}_q^{(i)} + R \sin \left(\theta - \frac{(i)}{\theta}_q \right)
\end{aligned} \tag{45}$$

in a common coordinate system (x,y) . The values of $\bar{x}_q^{(i)}$, $\bar{y}_q^{(i)}$, and $\frac{(i)}{\theta}_q$ for single fixed values of i and q may be chosen arbitrarily.

The framework provided by eqs. (10) - (45) now constitutes a complete system of recursion relations such that z_1 of the subsequent strip corresponds to z_2 of the present strip. Input data for this model requires prescription of the z - dependent radii, r_I , r_O , r_C , and r_S (usually given in digital fashion), M_q ($q = 1, 2$), the start-line meridian θ_S , and the helical angle ϕ at a single point on the start-line. In the event that no interleaving is present, one may simply neglect equations related to the region $q = 2$ or set $M_2 = M_1$ in the general equations. The start-line procedure always yields discontinuities in the ply pattern and the

involute surface unless an exact involute surface is employed. In the latter case, the start-line is no longer arbitrary and it is only necessary to use eqs. (1) - (9). If the exact involute surface is also cylindrical, then eqs. (41) and (42) can be used in place of (7) - (9).

EXPLICIT RELATIONS FOR THE START-LINE METHOD

In this section, we shall demonstrate that the equations defining involute parameters c_q , i.e., eqs. (12) - (14) and (17), can be solved in explicit (rather than iterative) fashion provided that we model the involute surface by strips of infinitesimal dimension $z_2 - z_1$.

Letting $z_1 = z$ and $z_2 = z + dz$, we observe that (14) may be expressed as

$$F_{S1}(z, z + dz) + \frac{A_1}{c_1} dz = 0 \quad (46)$$

while (11) gives

$$F_{S1}(z, z + dz) = \cot^2 \alpha_{S1} d\alpha_{S1} \quad (47)$$

where α_{S1} is the arc angle at $r_S(z)$. Now substituting (47) into (46) after use of (12) and its derivative leads to

$$A_1 dz = \frac{(r_S^2 - c_1^2)^{1/2} dr_S}{r_S} \quad (48)$$

whence, substituting (13) into (48) and solving for c_1 , we get

$$c_1^2 = \frac{1 + m_S^2}{4\pi^2/M_1^2 + m_S^2/r_S^2} \quad (49)$$

where

$$m_G = \frac{dr_G}{dz} \quad (50)$$

We also see that m_G is equivalent to $\tan \gamma_G$ by (4), however, the form (50) can be expressed in terms of given information, thus is more convenient for use in (49). Equation (49), which has been given earlier as a good first approximation for finite strip height $z_2 - z_1$, shows that c_1 in a practical exit cone built by the start-

line method never differs greatly from its value for cylindrical involutes ($\frac{M_1}{2\pi}$).

In similar fashion, we may derive an explicit expression for c_2 . In this case, (17) becomes

$$F_{C_2}(z, z+dz) - F_{C_1}(z, z+dz) = \left(\frac{A_1}{c_1} - \frac{A_2}{c_2}\right) dz \quad (51)$$

Using (11) and (12) along with its derivative again, we find that

$$\left[\frac{(r_C^2 - c_1^2)^{1/2}}{c_1} - \frac{(r_C^2 - c_2^2)^{1/2}}{c_2} \right] \frac{m_C}{r_C} = \frac{A_1}{c_1} - \frac{1}{c_2} \left(\frac{4\pi^2 c_2^2}{M_2^2} - 1 \right)^{1/2} \quad (52)$$

Solving for c_2 , we get

$$c_2 = \left(\frac{a_1 + a_2}{a_3} \right)^{1/2} \quad (53)$$

where

$$\begin{aligned} a_1 &= (1+m_C^2) (4\pi^2/M_2^2 + m_C^2/r_C^2) + (m_C^2-1)a_4^2 \\ a_2 &= 2m_C a_4 \left[(1+m_C^2) (4\pi^2/M_2^2 - 1/r_C^2) - a_4^2 \right]^{1/2} \\ a_3 &= (4\pi^2/M_2^2 - m_C^2/r_C^2 - a_4^2)^2 + 16\pi^2 m_C^2/M_2^2 r_C^2 \\ a_4 &= \frac{1}{c_1} \left[(4\pi^2 c_1^2/M_1^2 - 1)^{1/2} - (r_C^2 - c_1^2)^{1/2} m_C/r_C \right] \end{aligned} \quad (54)$$

The sign ambiguity in (53) is caused by an extraneous root resulting from the solution procedure. The correct root is the one that satisfies eq. (52). In order for a solution of (52) to exist, the input parameters must satisfy the relation

$$M_2 \leq 2\pi \left(\frac{1}{r_C} + \frac{a_4^2}{1+m_C^2} \right)^{-1/2} \quad (55)$$

which simply requires a_2 to be real. Also, if the region $q = 1$ is a cylindrical involute while $q = 2$ is not, the data must be such that $c_1 > c_2$.

Although the equations governing the ply pattern may be solved explicitly as above, the results are very cumbersome and inconvenient, thus they will not be derived here.

DISCONTINUITY STRAINS

An involute surface is conceived to be built of strips in the start-line approach. This hypothetical involute surface, in general, contains discontinuities in the form of "plateaus" at interfaces $z = \text{constant}$. Since the procedure is approximate it is important to quantify the error in order to compare ply patterns and to define regions in which ply pattern deformations tend to become excessive. Our proposed method of evaluation of ply pattern accuracy depends on the introduction of "discontinuity strains," which are defined as the components of an applied strain field that would transform the hypothetical involute surface into a continuous sheet.

We again consider a hypothetical involute surface generated by infinitesimal strips and its traces in the planes $z, z + dz = \text{constant}$. However, at $z + dz$, two traces are considered on the plateau. These correspond to involute constants c and $c + dc$ and are distinct except on the start-line, where the two traces intersect. In this way, we establish an algorithm suggested by Figure 5, where the six points 1-6 are introduced. Corresponding numerical values are used as subscripts to define coordinates. Points 1, 2, 3, and 4 all lie on a continuous surface with involute constant c , while 5 and 6 are on a surface defined by involute constant $c + dc$. The discontinuity strains are the (hypothetical) strains introduced in the transformation removing the discontinuity, i.e., moving 3 to 5 and 4 to 6.

In general, the discontinuity strains will not represent the actual strain field in the fabricated body since their presence

would depend upon specific (artificial) constraints. However, we may state that a continuous involute surface would result from their application. The discontinuity strains are a direct measure of the errors involved in the use of the start-line method, and they may be useful in delineating potential areas of wrinkling and severe fabric distortion. Thus, the discontinuity strains ϵ_{ij} should be considered as a guide to good ply pattern design, rather than as a precise measure of material deformation.

Recalling eq. (19), we can observe that

$$d\theta = \cot^2 \alpha d\alpha \quad (56)$$

and

$$dz = -\frac{c}{A} \cot^2 \alpha d\alpha \quad (57)$$

where the region index q is dropped since it is immaterial for the present analysis. Thus from (56), (57), and (12), we arrive at

$$\begin{aligned} r_2 &= r_1 - \frac{cd\theta}{\cos\alpha_1} \\ r_3 &= r_1 + \frac{Adz}{\cos\alpha_1} \\ r_4 &= r_1 - \frac{cd\theta}{\cos\alpha_1} + \frac{Adz}{\cos\alpha_1} \end{aligned} \quad (58)$$

where $\theta_1 = \theta_3 = \theta$ and $\theta_2 = \theta_4 = \theta + d\theta$.

It is now necessary to define the location of points 5 and 6 such that we maintain a one-to-one correspondence between themselves and their associated points 3 and 4. To accomplish this, we observe that, despite the appearance of two traces at $z+dz$, the radii at the end points of the two traces (r_0 and r_1) are identical since r_G are functions of z only. Thus, the ratio of arc lengths along the two traces is inversely proportional to the ratio of their involute constants. This relationship can be preserved by taking

$$r_5 = r_3 \quad (59)$$

$$r_6 = r_4$$

Thus, the transition between the traces at $z+dz$ involves a change in α , but not r . Using (12) then, we get

$$\frac{d\alpha}{dc} = \frac{\tan\alpha}{c} \quad (60)$$

at $z+dz$, while at the same level, we have

$$\frac{d(\alpha + \cot\alpha)}{dc} = -\frac{dc}{c} \cot\alpha = -\frac{dc}{c^2} (r^2 - c^2)^{\frac{1}{2}} \quad (61)$$

Substituting these relations into (19) leads to

$$\theta_5 = \theta + d\beta \quad (62)$$

where

$$d\beta = \frac{dc}{c^2} [c \cot\alpha_1 - (r_F^2 - c^2)^{\frac{1}{2}}] \quad (63)$$

and r_F is the radius at the point where the traces at $z+dz$ intersect, which is r_S if $q = 1$ and r_C if $q = 2$. We also get

$$\theta_6 = \theta_5 + d\theta \quad (64)$$

from (60), (61), and (19).

To define the discontinuity strains, we begin by computing the vectors \bar{s}_2 , \bar{s}_3 , and \bar{s}_5 that are directed from point 1 to the respective points as shown in Figure 5. In terms of a unit triad $(\hat{i}, \hat{j}, \hat{k})$ directed from the origin toward point 1, we have

$$\begin{aligned} \bar{s}_2 &= (r_1 \hat{i} - \frac{c}{\cos\alpha_1} \hat{j}) d\theta \\ \bar{s}_3 &= (\frac{A}{\cos\alpha_1} \hat{j} + \hat{k}) dz \\ \bar{s}_5 &= r_1 d\beta \hat{i} + \frac{Adz}{\cos\alpha_1} \hat{j} + dz \hat{k} \end{aligned} \quad (65)$$

where we have dropped higher order terms and δ is given by (63). Thus, the strain in the meridional direction (see Figure 6) is given by

$$\epsilon_m = \frac{s_5}{s_3} - 1 \quad (66)$$

which, on use of (65) and the assumption that $\epsilon_m \ll 1$, yields

$$\epsilon_m = \frac{(c \beta' \cot \alpha_1)^2}{2(A^2 + \cos^2 \alpha_1)} \quad (67)$$

where the prime denotes differentiation with respect to z . We note that β' can be expressed as

$$\beta' = \frac{c'}{c} [c \cot \alpha_1 - (r_F^2 - c^2)^{\frac{1}{2}}] \quad (68)$$

with c' given by differentiation of (49) or (53), according as $q = 1$ or 2 , respectively.

We now consider the strain in the s -direction, where s corresponds to the tangent vector in a plane normal to the z -axis. The appropriate deformation involves a transformation that carries the arc connecting points 3 and 4 into that connecting 5 and 6. The ratio of these two arcs, however, is the inverse of the ratio of their respective involute constants, which are c and $c+dc$. Hence, only infinitesimal strain accompanies this transformation and

$$\epsilon_s = 0 \quad (69)$$

For our third deformation measure, we shall compute the distortion of surface angle ψ . Letting Ω represent the angle between \bar{s}_2 and \bar{s}_5 , we get

$$\cos \Omega = \frac{\bar{s}_2 \cdot \bar{s}_5}{s_2 s_5} \quad (70)$$

which, on substitution of (65), becomes

$$\cos \Omega = \frac{(c \beta' \cot^2 \alpha_1 - A) \sin \alpha_1}{[(c \beta' \cot \alpha_1)^2 + A^2 + \cos^2 \alpha_1]^{1/2}} \quad (71)$$

Using elementary trigonometric relations in conjunction with (5) brings us to

$$\sin(\psi_1 - \Omega) = \frac{\{(A^2 + 1)^{1/2} (c \beta' \cot^2 \alpha_1 - A) + A[(A + c \beta')^2 + 1]^{1/2}\} \sin \alpha_1 \cos \alpha_1}{(A^2 + \cos^2 \alpha_1)^{1/2} [(c \beta' \cot \alpha_1)^2 + A^2 + \cos^2 \alpha_1]^{1/2}} \quad (72)$$

The quantities given by eqs. (67), (69), and (72) may be viewed as deformation measures in a non-orthogonal coordinate system since the angle between s and m is ψ , rather than $\pi/2$. These quantities may be transformed into discontinuity strains in the orthogonal system (s, t) shown in Figure 6 via the relations

$$\epsilon_m = \epsilon_t \sin^2 \psi_1 + \gamma_{st} \sin \psi_1 \cos \psi_1 \quad (73)$$

$$\Omega - \psi_1 = \epsilon_t \sin \psi_1 \cos \psi_1 - \gamma_{st} \sin^2 \psi_1$$

since the material on the s -axis does not deform or rotate (we have assumed that points 1 and 2 are fixed in space). Inverting (73) and repeating (69), we arrive at

$$\epsilon_s = 0$$

$$\epsilon_t = \epsilon_m + (\Omega - \psi_1) \cot \psi_1 \quad (74)$$

$$\gamma_{st} = \psi_1 - \Omega + \epsilon_m \cot \psi_1$$

The terms involving $\cot \psi_1$ tend to be small in practical exit cones since ψ is only slightly larger than $\pi/2$. The strains (74) may now be transformed into arbitrary coordinate systems, such as the warp/fill axes, by use of the standard strain transformation equations of linear elasticity.

DEBULKING KINEMATICS

In this section we shall derive explicitly the equations referred to in [1] pertaining to the analysis of debulking kinematics. Specifically, we shall consider the configuration of the involute surface corresponding to material in its initial, undebulked form assuming that the ply pattern based upon cured thickness is given, starting with the premise that it is desirable to pressurize against tooling that controls the profile of either final surface, i.e., $r_I(z)$ or $r_O(z)$, during debulk. The treatment is valid specifically for exact involute construction. Therefore, if involute construction based upon the start-line method is employed, the model given here applies strictly to a strip of the hypothetical involute surface.

As discussed in [1], it is not possible to design a ply pattern for an arbitrary body of revolution such that one of its edges will remain in contact with a control surface throughout a debulking procedure. However, approach was shown that permits an edge of the ply pattern to lie quite close to the control surface during debulking over a significant region provided that the ply pattern contains no discontinuities in the region. In this approach, the two end points of the ply pattern boundary in the (smooth) region, which are termed reference points, lie on the control surface. The formulation proceeds as follows:

Determine the ply pattern corresponding to the final (cured) state in the usual manner. We let the initial (undebulked) position

of point 1 coincide with its final location, while point 2 is merely constrained to lie on the control surface. The coordinates and other parameters evaluated at points 1 and 2 shall be denoted by the respective subscripts.¹ The usual notation is employed for the cured configuration, while the same symbols with asteriks will be used to refer to undebulked configuration. For the first approximation, let the initial coordinates $(r_2^*, \theta_2^*, z_2^*)$ coincide with their final values. Using (19) then, we arrive at

$$\theta_2^* - \theta_1 = \frac{A^*}{c^*} (z_2^* - z_1) + \alpha_1^* + \cot \alpha_1^* - \alpha_2^* - \cot \alpha_2^* \quad (75)$$

for a first approximation of c^* . Equation (75) can be solved by iteration starting with an assumed value

$$c^* \cong \frac{t^*}{t} c \quad (76)$$

Now let the control surface be defined by

$$r_2^* - r_1 = f(z_2^* - z_1) \quad (77)$$

where f is a known function. Also let ℓ represent the distance between the images of points 1 and 2 in the ply pattern, or

$$\ell^2 = R_1^2 + R_2^2 - 2R_1R_2 \cos(\theta_2 - \theta_1) \quad (78)$$

We then solve for r_2^* and z_2^* by iteration using

$$\theta^* = \frac{(z_2^* - z_1)(A^*)^2}{c^*[(A^*)^2 + 1]^{\frac{1}{2}}} - \lambda_2^* - \cot \lambda_2^* + \lambda_1^* + \cot \lambda_1^* \quad (79)$$

and

$$(R_1^*)^2 + (R_2^*)^2 - 2R_1^*R_2^* \cos \theta^* = \ell^2 \quad (80)$$

1 Similar to the previous section, numerical subscripts are only used in this section to denote the reference points 1 and 2 since the region index q is not needed. This assumes that points 1 and 2 are in the same region. Also, quantities with asteriks in this section represent the undebulked configuration and should not be confused with the previous meaning of the asteriks.

and (77). A good first approximation is $z_2^* = z_2$. The constant c^* can be adjusted for a closer fit between the initial ply boundary and the control surface. In this case, a revised solution of (77), (79), and (80) must be executed, while θ_2^* is given by (75).

At this time, we have the coordinates of each reference point. We also have the mapped image of each reference point in two coordinate systems. Thus, the next step is to establish the relationship between the two coordinate systems such that the two images of each reference point will coincide. Referring to Figure 7, this is accomplished by use of

$$\tan \bar{\theta} = \frac{ST^* - TS^*}{SS^* + TT^*} \quad (81)$$

where

$$\begin{aligned} S &= R_2 \cos \theta_2 - R_1 \cos \theta_1 \\ T &= R_2 \sin \theta_2 - R_1 \sin \theta_1 \end{aligned} \quad (82)$$

as well as

$$\bar{x} = R_1 \cos \theta_1 - R_1^* \cos (\theta_1^* - \bar{\theta}) = R_2 \cos \theta_2 - R_2^* \cos (\theta_2^* - \bar{\theta}) \quad (83)$$

and

$$\bar{y} = R_1 \sin \theta_1 - R_1^* \sin (\theta_1^* - \bar{\theta}) = R_2 \sin \theta_2 - R_2^* \sin (\theta_2^* - \bar{\theta}) \quad (84)$$

Given an arbitrary image (R, θ) in the final (cured) state, therefore, we can define its counterpart (R^*, θ^*) in the undebulked state via

$$R^* = [(R \cos \theta - \bar{x})^2 + (R \sin \theta - \bar{y})^2]^{1/2} \quad (85)$$

and

$$\tan (\theta^* - \bar{\theta}) = \frac{R \sin \theta - \bar{y}}{R \cos \theta - \bar{x}} \quad (86)$$

Finally, we arrive at the undebulked coordinates (r^*, θ^*, z^*) from the relations

$$r^* = \left[\frac{(A^*R^*)^2}{(A^*)^2+1} - \left(\frac{c^*}{A^*}\right)^2 \right]^{\frac{1}{2}} \quad (87)$$

$$z^* = z_1 + \frac{c^*[(A^*)^2+1]^{\frac{1}{2}}}{(A^*)^2} (\theta^* - \theta_1^* + \lambda^* + \cot \lambda^* - \lambda_1^* - \cot \lambda_1^*) \quad (88)$$

$$\theta^* = \theta_1^* + \frac{A^*}{c^*} (z^* - z_1) + \alpha_1^* + \cot \alpha_1^* - \alpha^* - \cot \alpha^* \quad (89)$$

which are derived from (8), (9), and (2). By use of the present model, one can approximate quite accurately the condition that a ply boundary remains in contact with a fabrication tooling surface, provided the ply boundary contains no discontinuity in the region.

The above treatment defines the debulking kinematics of an exact involute body. For a body constructed by the start-line method, eqs. (75) - (89) are only valid within a strip of the hypothetical involute surface. Because of the inherent discontinuities in the hypothetical involute surface, however, the form of the most accurate approximate scheme to treat the debulking kinematics for a body generated by the start-line method is not evident. Therefore, these problems should probably be examined via a case by case analysis.

CONCLUDING REMARKS

Construction of bodies such as rocket nozzle exit cones by the involute method involves analytical modeling of various aspects of the fabrication procedure. Furthermore, the fabrication approach may involve the use of an exact involute ply pattern or one generated by the (inexact) start-line method, which may include interleaving. Since the start-line model contains inherent discontinuities, it is important to evaluate the effect of the approximation on ply pattern distortion and deformation. Finally, proper debulking requires carefully designed tooling and a model describing the kinematics of the debulk process. Aside from the manufacturing considerations, the stress analyst needs a model to characterize the variation of the important involute parameters, such as arc and helical angles, throughout the body, as these parameters define the distribution of the elastic stiffness tensor, which in turn influence the stress field. All these topics have been treated here including the development of explicit relations where practical. Although some of these equations appear elsewhere, such as [1] - [4], they have also been included here for completeness and convenience of the reader.

REFERENCES

1. Pagano, N.J., "Exact Involute Bodies of Revolution," Journal of the Engineering Mechanics Division of the American Society of Civil Engineers, 1982, pp. 255-276.
2. Stanton, E.L. and N.J. Pagano, "Curing Stress Fields in Involute Exit Cones" Modern Developments in Composite Materials and Structures, J.R. Vinson, ed.. The American Society of Mechanical Engineers, New York, 1979, pp. 189-214.
3. Savage, E.E., "The Geometry of Involute Construction," JANNAF Rocket Nozzle Technology Subcommittee Meeting 1979, CPIA Publication 310, 1980 pp. 293-308.
4. Stanton E.L., J.G. Crose, F. Inman, and W. Prescott, "Design and Analysis of the IPSMII Carbon-Carbon Involute Exit Cones", 1981 JANNAF Rocket Nozzle Technology Subcommittee Meeting, CPIA Publication 346, 1981 pp. 223-236.

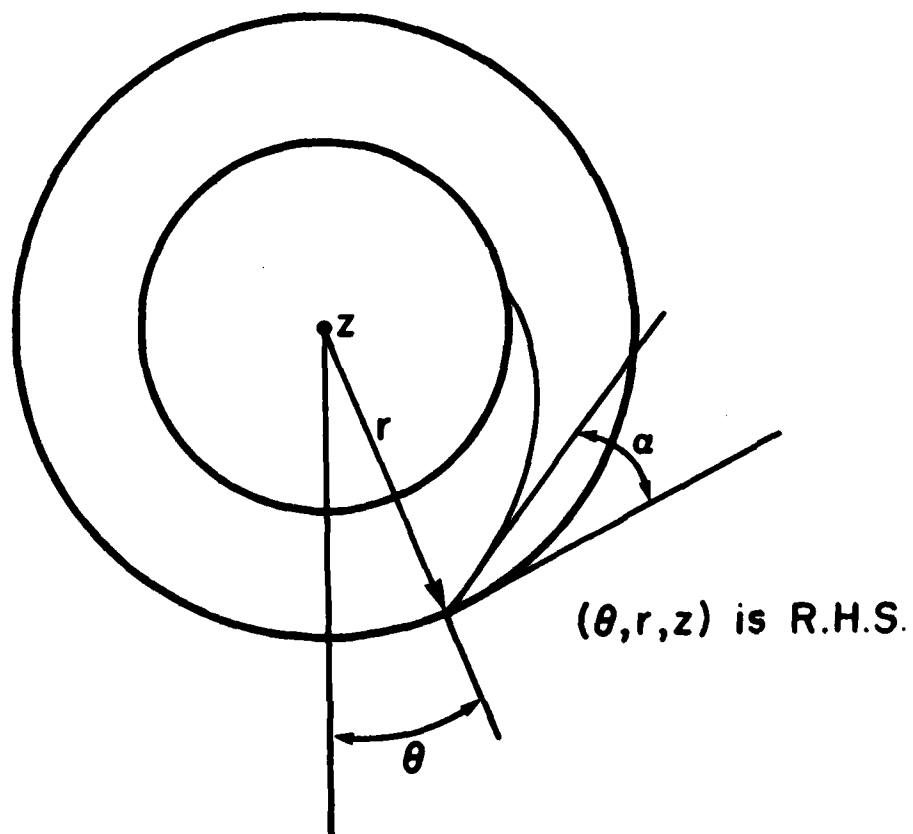


Figure 1. Involute Surface Coordinate System.

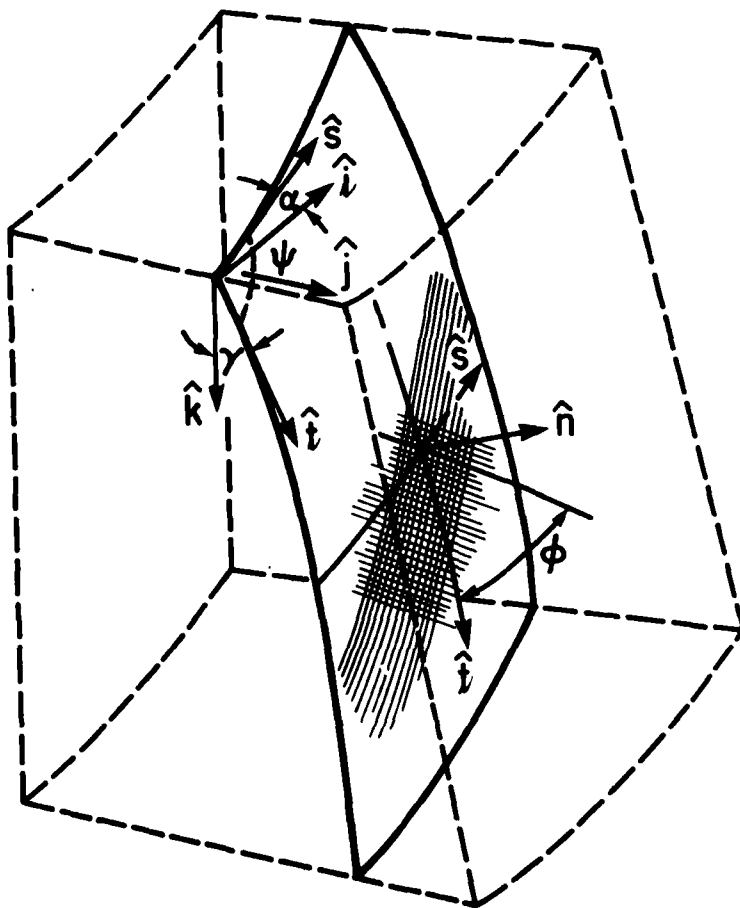


Figure 2. Involute Surface Geometry.

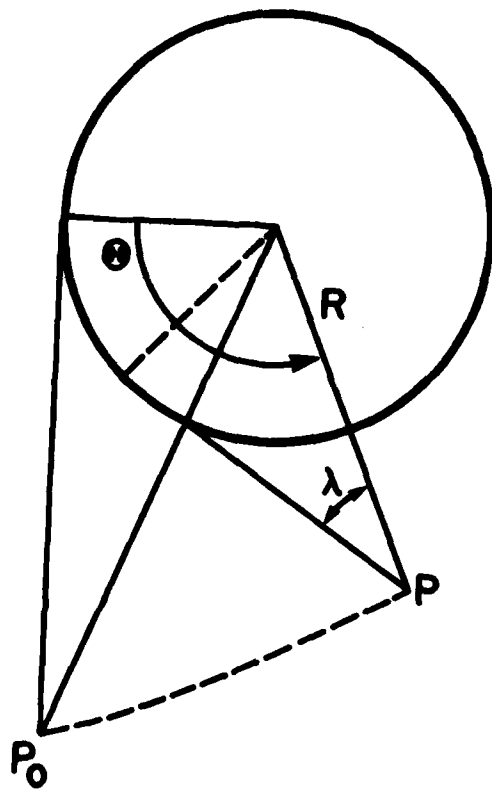


Figure 3. Ply Pattern Coordinates.

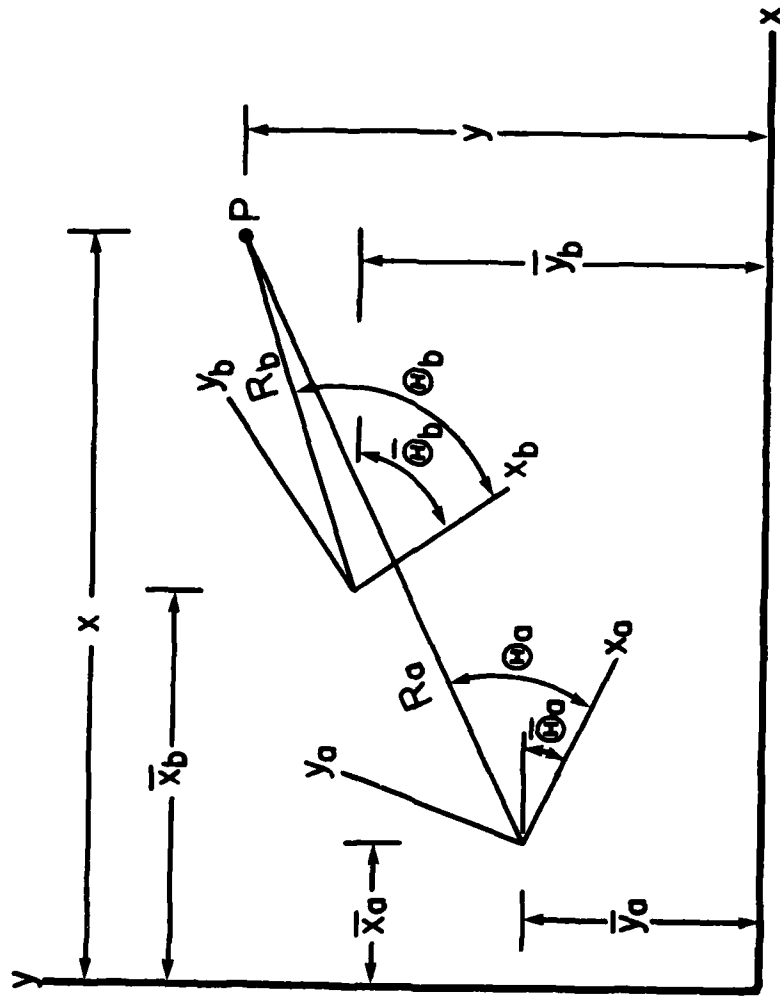


Figure 4(a). Transformation of Ply Pattern Coordinates.

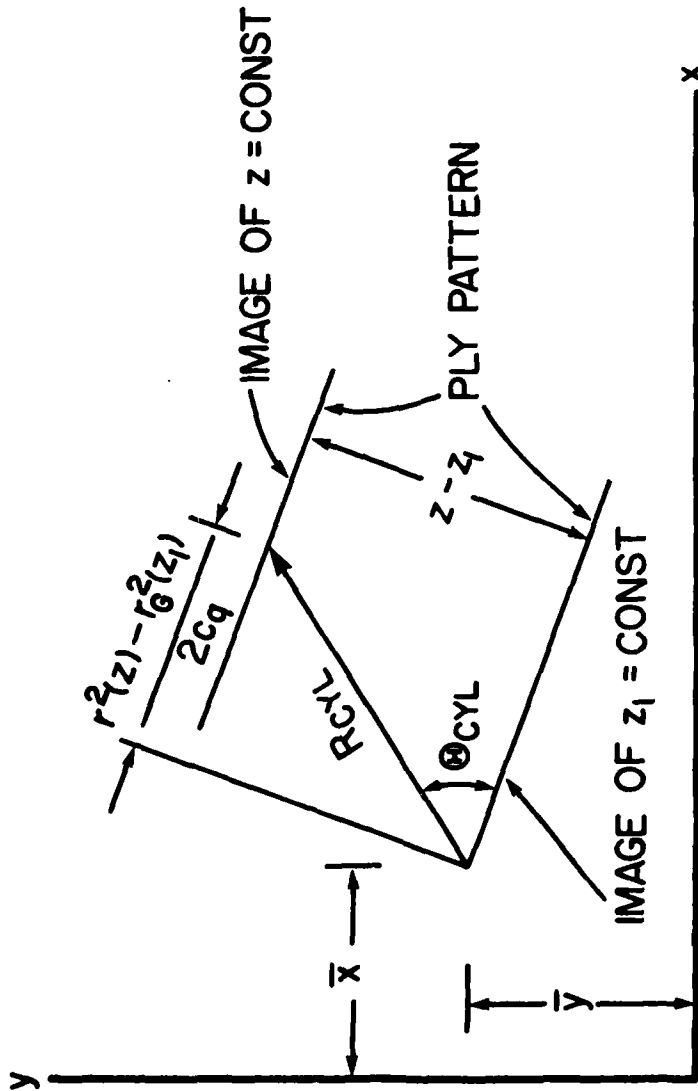


Figure 4(b). Definition of Cylindrical Involute Ply Pattern Coordinates.

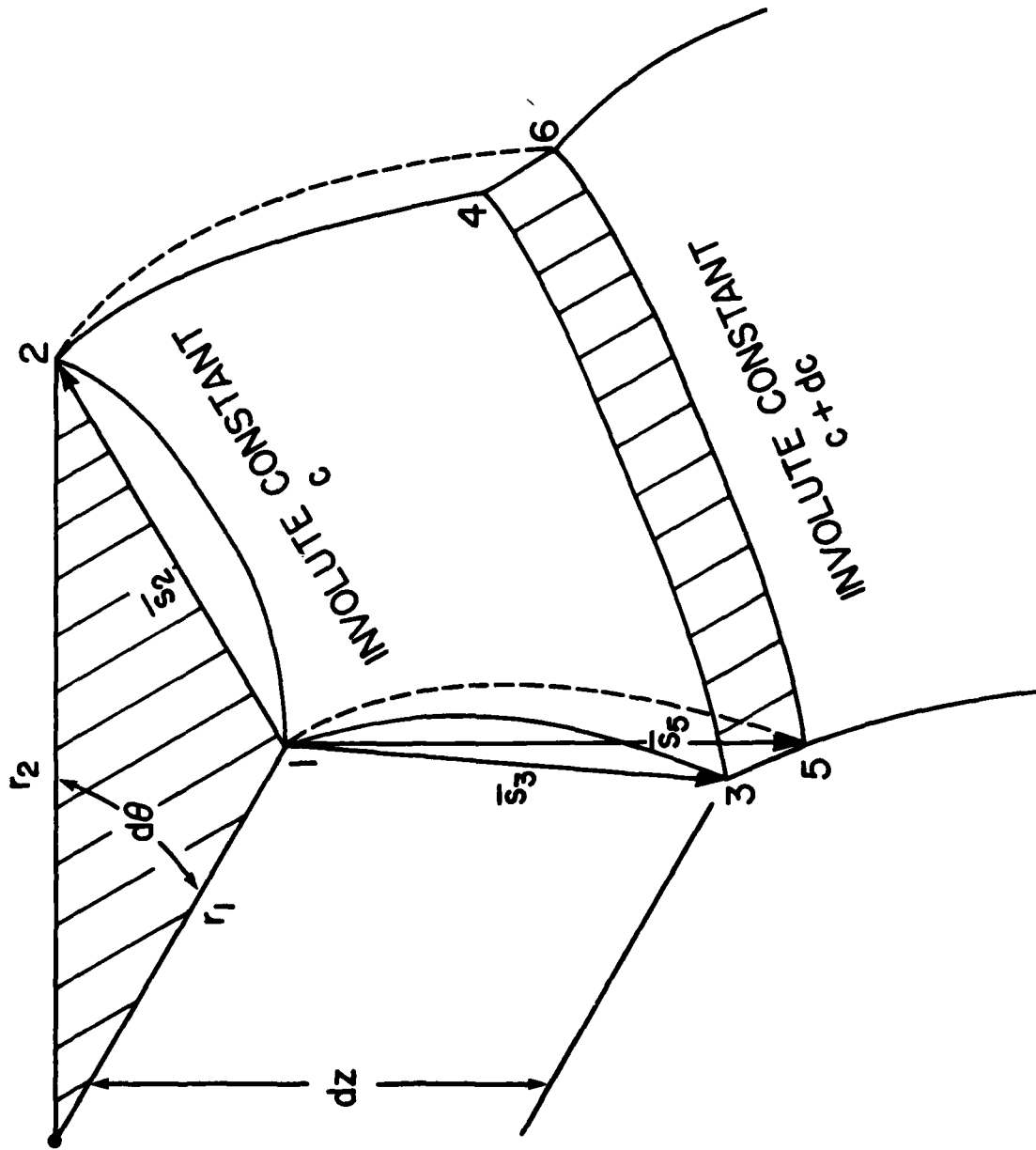


Figure 5. Discontinuity Produced in the Start-Line Approach.

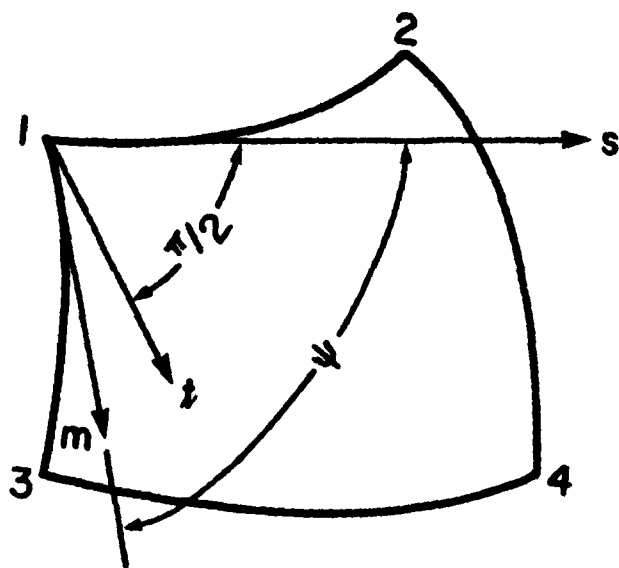


Figure 6. Coordinate Axes for Discontinuity Strains.

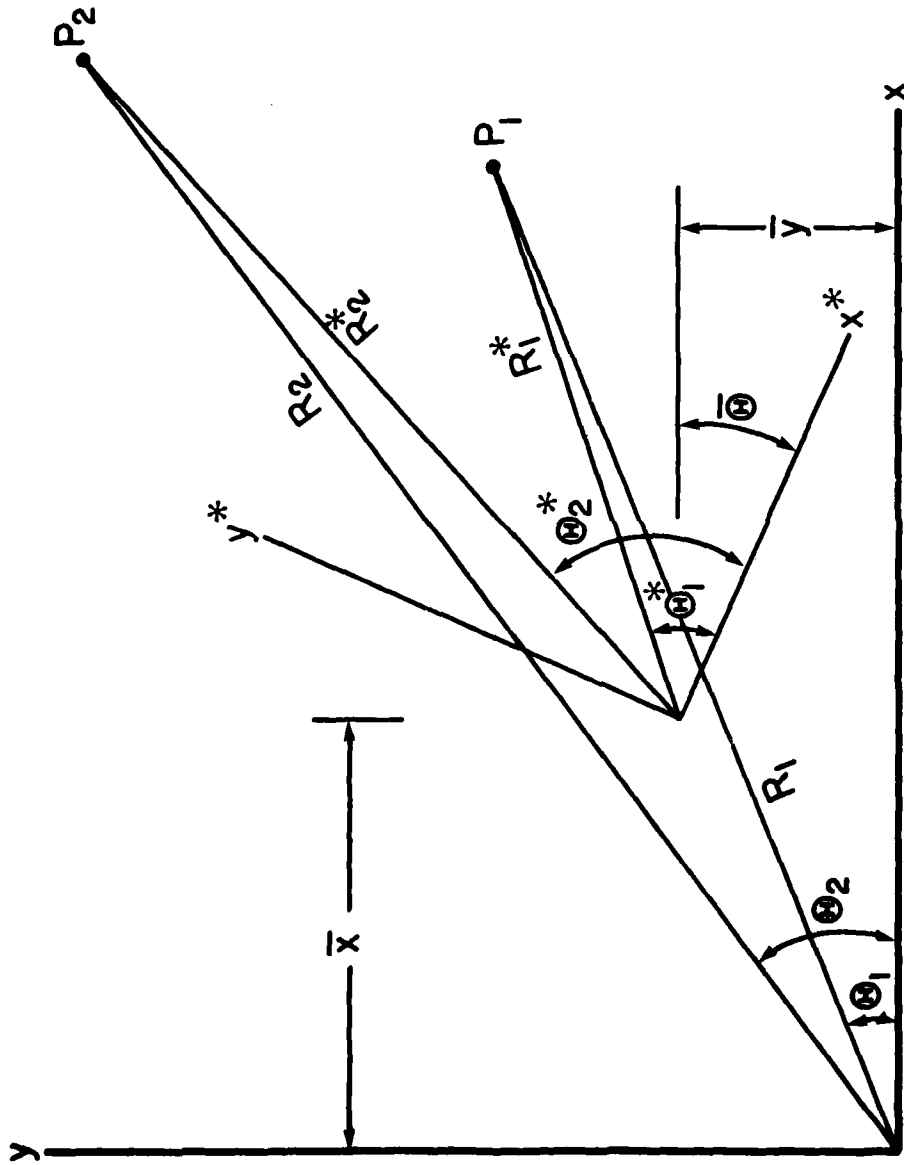


Figure 7. Transformation for Debulk Analysis.

APPENDIX A

A NOTE ON SIGN CONVENTIONS

Since many parameters are involved in the definition of the exact involute surface, it is not surprising that various sign conventions appear in the literature. In other cases, inconsistencies in sign are present, e.g., eq. (B-3) of [1] and eq. (3) of [2]. These have been corrected in the corresponding equations of the present work. Since the use of these relations to define stiffness, stress, and displacement components in stress field models requires rigid adherence to a consistent sign convention, we shall review the present nomenclature in explicit fashion at this point.

All equations derived in this work are consistent with the following convention:

- a) Unit vectors $\hat{i}, \hat{j}, \hat{k}$ lie in the directions of (increasing) θ, r, z , respectively. The unit vectors $\hat{i}, \hat{j}, \hat{k}$, in that order, form a right-hand triad. Furthermore, the involute surface is assumed to be oriented such that the slope of the meridian, $\frac{dr}{dz}$, is not negative.
- b) Unit vectors $\hat{t}, \hat{s}, \hat{n}$ must be oriented such that they are defined by

$$\begin{aligned}\hat{t} &= \hat{j} \sin \gamma + \hat{k} \cos \gamma \\ \hat{s} &= \hat{i} \cos \alpha - \hat{j} \sin \alpha \\ \hat{n} \sin \psi &= \hat{t} \times \hat{s}\end{aligned}\tag{A-1}$$

and the ranges of the various angles are given by

$$0 \leq \alpha \leq \pi/2, \quad 0 \leq \gamma \leq \pi/2, \quad \pi/2 \leq \psi \leq \pi\tag{A-2}$$

In this way, \hat{n} is the unit outward normal vector of the involute surface.

c) The helical angle ϕ may be chosen to represent the orientation of any particular line segment on the ply pattern. For definiteness, let us assume ϕ is measured to the warp direction. Then a positive angle ϕ is measured from the meridian toward the warp direction such that the vector representing ϕ by the right-hand rule lies in the direction of \hat{n} .